EXPERIMENTAL CELL RESEARCH 241, 285–299 (1998)
ARTICLE NO. EX984031

608

Regulation of Protrusion Shape and Adhesion to the Substratum during Chemotactic Responses of Mammalian Carcinoma Cells

Maryse Bailly,*[,1] Lin Yan,† George M. Whitesides,† John S. Condeelis,* and Jeffrey E. Segall*

*Department of Anatomy and Structural Biology, Albert Einstein College of Medicine, 1300 Morris Park Avenue, Bronx, New York 10461; and †Department of Chemistry and Chemical Biology, Harvard University, 12 Oxford Street, Cambridge, Massachusetts 02138

We report here the first direct observation of chemotaxis to EGF by rat mammary carcinoma cells. When exposed to a gradient of EGF diffusing from a micropipette, MTLn3 cells displayed typical ameboid chemotaxis, extending a lamellipod-like protrusion and moving toward the pipette. Using a homogeneous upshift in EGF to model stimulated lamellipod extension (J. E. Segall *et al.*, 1996, *Clin. Exp. Metastasis* 14, 61–72), we analyzed the relationship between adhesion and chemoattractant-stimulated protrusion. Exposure to EGF led to a rapid remodeling of the adhesive contacts on adherent cells, in synchrony with extension of a flat lamellipod over the substratum. EGF-stimulated lamellipods still extended in the presence of adhesion-blocking peptides or over nonadhesive surfaces. They were, however, slightly shorter and retracted rapidly under those conditions. The major protrusive structure observed on well-spread, adherent cells, after EGF stimulation was a flat broad lamellipod, whether or not in contact with the substratum, while cells in suspension showed transient protrusive activity over the entire cell surface. We conclude that the initial adhesive status of the cell conditions the shape of the outcoming protrusion. Altogether our results suggest that, although adhesive contacts are not necessary for lamellipod extension, they play a role in stabilizing the protrusion as well as in the control of its final shape and amplitude. © 1998 Academic Press

Key Words: chemotaxis; cancer cells; adhesion; protrusion; lamellipod extension.

INTRODUCTION

Epithelial cells are normally arranged as highly organized tissues of differentiated cells. During oncogenic progression, some of these cells are able to dedifferentiate, break adhesions with neighboring cells, and initiate movement out of the tumor into the surrounding stroma and blood vessels [1–3]. Tumor cell motility and protrusive activity are generally correlated with high invasive and metastatic potentials [4, 5]. Cytokines and growth factors acting through receptor tyrosine kinases, such as EGF, PDGF, or HGF/SF, have been shown to stimulate tumor cell motility and chemotaxis *in vitro* in assays as different as Boyden chambers, wound healing, or invasion of collagen matrices [6–10]. In addition, clinical studies suggest a direct involvement of the EGF receptor in the metastatic process during breast cancer progression [11–15]. Thus acquisition of cell motility and chemotactic ability could be a critical factor in tumor cell progression. The detailed biological as well as biochemical analysis of these processes remains, however, incomplete.

The chemotactic process has been studied in detail in ameboid cells such as *Dictyostelium* and neutrophils, and part of the molecular mechanisms underlying this process has been revealed [16–18]. Those chemotactic responses, however, are typically mediated by G-protein-coupled receptors, and much less is known about the receptor tyrosine pathways regulating the directed motility of epithelial and mesenchymal mammalian cells. These cells have dramatically different cell morphologies and actin cytoskeletons when compared to the amoeboid phagocytes. In particular, most of the polymerized actin is organized into long, complex stress fibers which are anchored in focal contacts at the cell membrane. The process of cell movement in epithelial and mesenchymal cells is believed to involve extension of a lamellipod and formation of close contacts (and possibly focal contacts), followed by flow of cytoplasm into the lamellipod and retraction of the rear of the cell [for reviews see Refs. 16, 19, 20]. Studies in a variety of cell types with different extracellular matrix molecules have shown that movement of such cells is dependent upon an optimum level of adhesion [21–23]. Excessive adhesion may block release of old attachments and reduce motility [24, 25], while inhibition of cell–substratum adhesion will block cell attachment, spreading, or *in vitro* invasion through membranes and tissues [26–28]. Stimulation with chemoattractants or microinjection of the activated small GTPase rac can lead to ex-

[1] To whom correspondence and reprint requests should be addressed. Fax: (718) 430 8996. E-mail: bailly@aecom.yu.edu.

0014-4827/98 $25.00

tension of a thin, flat lamellipod parallel to the substratum [6, 29]. The dependence of cell spreading on adhesion to a surface and the presence of focal complexes at the tip of the extended lamellipod [29] raises the possibility that cell–substratum interactions may be important during cell spreading and lamellipod extension.

Studies of cell–substratum adhesion molecules, such as integrins [30–32], have demonstrated a number of mechanisms by which binding to extracellular matrix can affect cellular responses. Members of the integrin family can interact on the extracellular side with extracellular matrix while the cytoplasmic portions of the molecules have been found to couple to the actin cytoskeleton via proteins such as talin and α-actinin. In addition to providing a mechanical coupling between the extracellular matrix and the cytoskeleton, integrins have been found to activate intracellular signaling pathways as well [33, 34]. Some of these pathways may lead to actin polymerization [36–38]. Thus binding of cell surface receptors to matrix molecules could provide key signals for regulating or amplifying cellular motility events.

On the other hand, a number of detailed studies have dealt with the process of random motility, typically in fibroblasts [24, 39–41]. Phenomenological observations on such unstimulated fibroblasts have suggested that random protrusion can occur in a manner independent of adhesion to a substratum [39, 42–44]. While it was originally believed that the main steps in chemotaxis and random motility are the same, it now appears however that the signals that mediate chemotaxis can be distinct from those that regulate unstimulated random motility [9]. For example, mouse fibroblasts expressing activated tyrosine kinase genes can show completely independent alterations in their random motility, chemotactic, or chemokinetic properties toward PDGF [9]. Likewise, alterations of the cell/substratum contacts in CHO cells, through modulation of integrin receptors' ability to mediate cytoskeletal linkages and ligand affinity, can result in decreased haptotactic migration, while random motility is actually increased [45]. Chemotactic and haptotactic responses to vitronectin appear to involve different signaling pathways as well [46].

Therefore, an understanding of cell motility and chemotaxis at the molecular level requires a clear identification of the steps in the chemotactic response that require adhesion. During which steps in the chemotactic response are adhesive interactions important? Can the protrusive phase be separated from the adhesive phase? Chemotactic migration of adherent cells has mostly been studied with long-term indirect assays (spanning over hours), using Boyden or microchemotaxis chambers [47, 48] that do not provide a morphological analysis of cell motility. Such end-stage experiments do not easily sort out the contributions of adhesion, cell–cell contact, motility, or even new protein synthesis. Although useful for testing a number of samples at once, the Boyden chamber technique suffers from the drawback of relatively poor time resolution. At the cellular level, responses to the addition of chemoattractant occur within 1 min, while with the Boyden chamber, several hours (corresponding to many cycles of cell movement) are required to get a strong response [49]. In addition, the use of such methods to define chemotactic responses to growth factors has also been questioned due to the possibility of autocrine secretion of other motility factors during such prolonged assays [50]. Therefore, a method with higher time resolution for dissecting the chemotactic response is necessary to more precisely define true chemotaxis and the role of adhesion in this event. This will prove particularly important for understanding the mechanisms of tumor cell migration and metastasis [1–3].

Rapid addition of a chemoattractant to responsive cells has provided a convenient method to synchronously generate the process of lamellipod extension in a large number of cells with a defined time course [6, 51]. The stimulus can be delivered relatively quickly, and then rapid cell responses can be easily quantified under a variety of experimental manipulations. This assay then provides a means to directly test the relationships between adhesion and protrusion in chemoattractant-stimulated lamellipod extension. Utilizing such an assay, this report describes the first comprehensive direct analysis, using high temporal and spatial resolution, of the regulation of protrusive activity during chemotactic responses of adherent cells. We have used a well-characterized rat mammary adenocarcinoma cell line which has been shown previously to display chemotactic activity toward EGF in the modified Boyden chamber assay [6]. We demonstrate here that these cells display classical ameboid chemotaxis on a plane surface in response to a point source of EGF. While the EGF-stimulated protrusive activity is shown to be independent of any contact with the substratum, we show that the shape as well as the magnitude of the protrusion is dictated by the relationship between the cell and the substratum prior to any stimulation.

MATERIAL AND METHODS

Cells. MTLn3 metastatic rat mammary adenocarcinoma cells were kindly provided by Dr. Garth Nicholson, MD Anderson Cancer Center, Houston, Texas. Cells were grown in α-MEM (Gibco), supplemented with 5% fetal calf serum and antibiotics as previously described [6]. For all experiments, unless otherwise mentioned, MTLn3 cells were prepared as follows: cells were plated in regular medium for about 24 h at low density on tissue culture dishes (Falcon), MatTek dishes (MatTek Corporation, Ashland, MA), or regular or patterned (see below) coverslips, which had been previously coated for 2 h at room temperature with rat collagen I (Collaborative Biochemicals) at 30 μg/ml in DPBS (Gibco). They were starved for 3 h

prior to the experiment in α-MEM medium supplemented with 0.35% BSA and 12 mM Hepes (starvation medium). Stimulation was done with a final concentration of 5 nM murine EGF (Life Technologies) in starvation medium.

Antibodies. Anti-talin monoclonal antibody clone 8d4 was purchased from Sigma. Rabbit anti-bovine vitronectin was purchased from Gibco. Cy5-conjugated goat anti-mouse IgG was purchased from Accurate Laboratories and Scientific Corporation. Fluorescein-conjugated goat anti-mouse IgG and goat anti-rabbit IgG were purchased from Cappel Laboratories.

Chemotaxis assay. Starved MTLn3 cells in tissue culture dishes were viewed with a Nikon Diaphot microscope in a temperature chamber at 37°C. Micropipettes were made from capillary tubing (A-M Systems, No. 6010) pulled on a Narishige PB-7 puller. They were filled with 50 μM EGF in DPBS and mounted in a Narishige MN-151 micromanipulator. The micropipette was lowered to about the level of the cells and phase contrast images were recorded simultaneously on videotape and on a Macintosh Quadra for an average time of 30 min. The movies were assembled using NIH Image and analyzed with the 2D-DIAS program (Solltech, Iowa City, IA) to generate the corresponding difference movies. The cell speed was inferred from the total distance crawled by the cell divided by the total time, and the chemotaxis index was calculated as the ratio of the net movement toward the pipette to the total cell movement [52]. Two aspects of this experiment are critical for successful observation of cell movement toward the pipette. First a relatively high concentration of EGF (50 μM or 10,000 times the concentration necessary for full lamellipod extension) is necessary in the micropipette due to the large dilution occurring during diffusion from the tip. Second, serum starving cells (with BSA to preserve osmotic balance) provides the optimum degree of sensitivity and may reduce the presence of compounds which can plug the pipette tip. Control experiments were done with DPBS only in the pipette.

Lamellipod extension assay. Lamellipod extension was evaluated as an overall increase in the total area of the cells as previously described [6]. Briefly, starved cells in tissue culture dishes or on patterned coverslips (see below) were transferred to a microscope chamber heated at 37°C. Cells were then stimulated with EGF, and phase contrast images were recorded every 1 min. The movies were assembled using NIH Image and measurements of the area, or other relevant parameters (maximum length, maximum width, central width), for each cell were done using 2D-DIAS. For experiments done in the presence of peptides, MTLn3 cells were starved for 3 h and detached with 5 mM EDTA in DPBS. The cells were then plated for 2 h in starvation medium on dishes previously coated with rat vitronectin (Sigma) at 10 μg/ml for 1 h at room temperature. Ten minutes prior to the beginning of the experiment, the medium was removed and replaced by fresh starvation medium for peptide-free control or starvation medium containing 3 mM GRGDSP inhibitory or GRADSP control peptides (Gibco). Cells were stimulated by addition of an equal volume of 10 nM EGF in starvation medium so that the final concentrations for the peptides and EGF were, respectively, 1.5 mM and 5 nM. For comparative purposes, the results in this experiment were expressed as normalized area, by dividing the values for the area by the average prestimulus value [6].

IRM studies of live cells. Cells on MatTek culture dishes were transferred to a microscope chamber heated at 37°C. Dishes were viewed under IRM with an IX70 Olympus Microscope and cells were then stimulated with a final concentration of 5 nM EGF. Time-lapse images were recorded every 30 s with a cooled CCD camera coupled to a Macintosh Power PC. Movies were then assembled using NIH Image.

Preparation of patterned coverslips. The patterned coverslips were prepared according to a previously described procedure [53]. Briefly, a 10:1 (w/w) mixture of Sylgard Silicone Elastomer 184 and Sylgard Curing Agent 184 (Dow Corning Corp., Midland, MI) was cast over a master, which was generated by photolithography, and pressure degassed. After sitting at room temperature for 30 min, the PDMS was cured at 60°C for 1 h. The stamp was carefully peeled off the master after cooling to room temperature and rinsed with ethanol. The PDMS stamp was inked by a cotton swab which has been moistened with a 1 mM solution of hexadecanethiol ($CH_3(CH_2)_{15}SH$; purchased from Aldrich and purified by flash chromatography prior to use) in ethanol. The resulting stamp was placed on the gold substratum (125 Å gold on a titanium-primed 24 × 50-2 microscope coverglass) and gentle hand pressure was applied to aid in complete contact between the stamp and the substratum. After 30 s, the stamp was peeled off the substratum and the coverslip was immersed directly in a 2 mM solution of (1-mercaptoundec-11-yl)hexa(ethylene glycol) ($HO(CH_2CH_2O)_6(CH2)_{11}SH$; prepared according to the procedure of Prime and Whitesides, Ref. [54]) in ethanol. After approximately 2 h of immersion, the coverslip was removed from the solution, rinsed with ethanol, and dried with a stream of nitrogen.

Immunofluorescence studies. Cells were plated on coverslips or MatTek dishes and stimulated with EGF or left untreated. They were fixed for 5 min at 37°C with 3.7% formaldehyde in a buffer containing 5 mM KCl, 137 mM NaCl, 4 mM $NaHCO_3$, 0.4 mM KH_2PO_4, 1.1 mM Na_2HPO_4, 2 mM $MgCl_2$, 5 mM Pipes pH 7.2, 2 mM EGTA, pH 7, and 5.5 mM glucose (stabilization buffer). Permeabilization was done for 20 min at room temperature in 0.5% Triton X-100 in stabilization buffer. The cells were then rinsed once with 0.1 M glycine in stabilization buffer and incubated for an additional 10 min in glycine. After five washes with TBS, pH 8, the preparations were blocked/stained for F-actin by incubation for 20 min with 0.5 μM rhodamine-labeled phalloidin (Molecular Probes) in TBS, pH 8, supplemented with 1% BSA and 1% fetal calf serum. For double labeling with talin, cells were incubated for an additional 1 h with anti-talin antibody followed by five rinses in TBS plus 1% BSA and incubation for 1 h with fluorescein-labeled anti-mouse IgG. After final washes, the coverslips were mounted in 50% glycerol in TBS supplemented with 6 g/liter *N*-propyl gallate. For experiments on patterned coverslips, the cells were stained for F-actin as described above, and the lanes of adhesive substratum were visualized using an anti-bovine vitronectin antibody followed by a FITC-conjugated goat anti-rabbit IgG. For experiments in suspension, MTLn3 cells starved for 3 h were detached with EDTA, resuspended in starvation medium at a concentration of 3×10^6 cells/ml, and placed at 37°C for 10 min to recover. The cells were then stimulated with 5 nM EGF, and samples were taken different times after suspension to be immediately fixed with 3.7% formaldehyde in stabilization buffer for 5 min at 37°C. One-hundred microliters of fixed cells was then added to coverslips previously coated with 0.05% polyethylenimine, and the cells were allowed to adhere for 8 min. The coverslips were then washed for 5 min in PBS and processed for F-actin staining as described above.

For focal contact quantitation, cells were double labeled for F-actin and talin as described above. The number and size of talin-containing focal contacts were assessed in a representative number of cells at different times after stimulation using NIH Image on images obtained from single optical 0.5-μm-thick sections taken with a Bio-Rad MRC-600 confocal microscope. For 3D reconstructions, a Bio-Rad MRC-600 confocal microscope was used to generate Z-series at 0.285-μm steps, and three-dimensional reconstructions were done using VoxelView (Vital Images, Inc.)

Quantitation of protrusive activity. Quantitation of protrusive activity in suspension was done using DIC optics on a Nikon Diaphot microscope on preparations prepared for F-actin staining as described above. Cells presenting one or more protrusions were scored as positive for protrusion. Quantitation of dorsal protrusive activity was done using fluorescence optics on a Nikon Diaphot microscope on coverslips or MatTek dishes prepared for F-actin staining. Cells presenting significant protrusive activity (at least one large ruffle or three small protrusions) on their dorsal surface were scored as positive in this assay.

RESULTS

Metastatic Cells Display Direct Ameboid Chemotaxis to EGF

MTLn3 cells are chemotactic toward EGF as measured indirectly in the microchemotaxis chamber assay [6]. However, indirect and long-term assays such as the microchemotaxis chamber leave open the possibility that growth factors stimulate the secretion of autocrine factors which in turn are the true chemoattractants. The question has been raised as to whether any cell type is directly chemotactic to growth factors [50]. This can only be answered by direct observation of cell orientation to spatial gradients of chemoattractants, as has been established for more rapidly moving cells such as *Dictyostelium* and neutrophils [55]. To directly observe the chemotactic movement of MTLn3 cells, a micropipette stimulation assay was developed, based on assays utilized for studying *Dictyostelium discoideum* [56]. The gradient was generated by placing a pipette filled with a concentrated EGF solution next to individual MTLn3 cells. Figure 1A shows a representative video sequence of an MTLn3 cell that reoriented to follow changes in the position of the pipette (a link to the complete movie that was used to generate this figure is available, see Acknowledgments). Digital analysis of the movement showed that the cell maintained a fairly direct motion toward the micropipette (Fig. 1B), undergoing continuous protrusion at the front and retraction at the rear. When the pipette was moved, reorientation of the cell to follow the pipette was apparent within 2 min and the cell resumed linear motion in the new direction. This change in direction is shown as a net turn in the cell path (Fig. 1B, top left image). Protrusion occurred mainly by the extension of a broad, flat lamellipod in the direction of the pipette, with occasional ruffling at the leading edge. Figure 1C shows a complete reversal of cell polarity when the pipette was placed at the rear of a cell. The cells exposed to the gradient presented a high chemotactic index and moved approximatively twice as fast as the controls (Table 1). The rate of movement differed from one cell to another, appearing as an intrinsic characteristic of the cell, and was independent from the initial polarity of the cell; e.g. cells that had to reverse polarity to move toward the pipette were not slower crawlers (data not shown).

Regulation of Shape and Extent of Protrusion by Contact with the Substratum

We have shown previously that stimulation of MTLn3 cells with a homogeneous, sudden increase in the concentration of EGF (with no spatial gradient) results in the actin-dependent extension of a flat, broad lamellipod, similar to what was seen in the micropipette assay in Fig. 1 [6]. This effect is specific to EGF, since MTC cells (the nonmetastatic counterpart of MTLn3 cells, derived from the same original tumor but defective in EGF-receptor expression) do not show any response to EGF or TGF-α [6, 57]. Such a stimulus protocol has been shown to generate synchronized lamellipod extension in a large number of cells, which then provides adequate material for more detailed analysis [6]. We used this assay to explore the relationships between adhesion and protrusion during lamellipod extension.

Protrusions from regions that are not in contact with the substratum. Lamellipods induced by EGF in well-spread, isolated MTLn3 cells typically are extremely flat and extend parallel to the substratum [6]. Scanning electron microscope observations of stimulated MTLn3 cells confirm the light microscope observations [57]. This EGF-stimulated protrusive activity is accompanied by an increase in actin polymerization at the leading edge, resulting in an accumulation of F-actin at the leading edge within a few minutes [6, 58]. Using confocal microscopy and three-dimensional reconstruction of cells labeled for F-actin, we confirmed that this burst of actin polymerization dominated at the very edges of the spread lamella of the cells and did not involve the whole submembrane compartment of the cell (Fig. 2). A closer kinetic analysis of the cells after EGF stimulation revealed, however, transient protrusive activity on the dorsal surface over the central portion of some cells as well (Fig. 3). The fraction of adherent cells displaying actin-rich protrusions over their dorsal surface increased from 30% in unstimulated cells to a maximum of 50% 2 min after stimulation. This fraction then rapidly decreased with time, and by 3 min after stimulation only 15% of the cells showed protrusions. By 20 min after stimulation, the fraction of cells showing dorsal protrusive activity returned to the prestimulus value (data not shown). Thus, though the major outburst of protrusive activity is concentrated in the lamellipod, areas clearly not in contact with the substratum showed protrusive activity that was transiently stimulated by EGF. Furthermore, DIC images of unstimulated cells in suspension show that they appear round with relatively small protrusions (Fig. 4A). Two minutes after EGF stimulation, however, many cells display large actin-rich protrusions. By 5 min after stimulation, the amount as well as the size of the protrusions have decreased. High-resolution reconstruction of the F-actin cortical cytoskeleton showed that protrusions arose over the entire cell surface (Fig. 4B). The number of cells displaying protrusive activity, as observed with DIC, was maximal 2–3 min after EGF stimulation (Fig. 5; significant difference between the values at 2 and 5 min, $P = 0.05$. Student t test). Thus, MTLn3 cells are able to generate

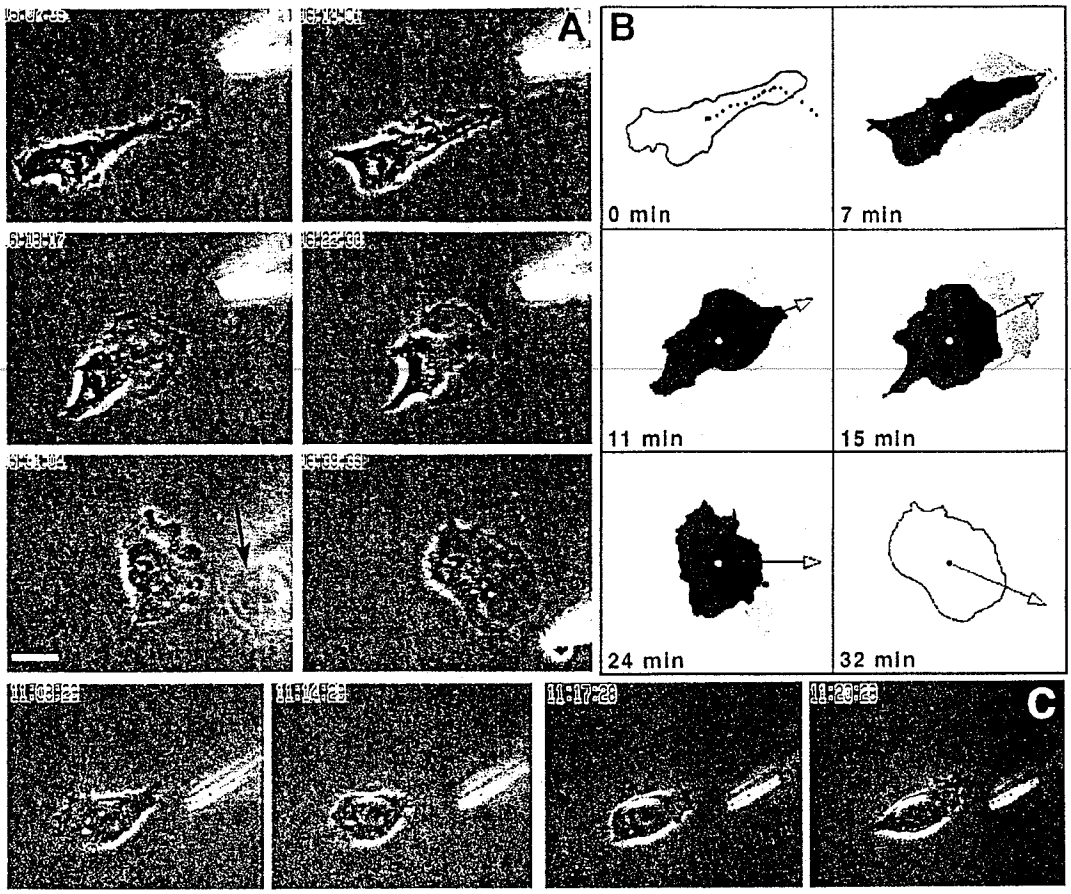

FIG. 1. Metastatic cells display ameboid chemotaxis. (A) An MTLn3 cell oriented toward a pipette filled with a solution of 50 μM EGF (time in the top left corner). The cell crawled toward the pipette and changed direction when the pipette was moved (arrow marks the moving pipette on image 16:31:04); bar, 20 μm. (B) Difference images showing lamellipod extension at the front of the cell (light gray) and retraction at the rear (medium gray). Time is indicated as minutes after initial positioning of the pipette. The cell path over the course of the experiment is shown as the position of the centroid of the cell once every minute on the top left image. (C) Typical reversal of polarity of a cell responding to the gradient of EGF.

EGF-stimulated protrusive activity in a substratum-free environment, and the shape of the resulting protrusions is similar to what was observed transiently on the dorsal surface of stimulated adherent cells.

TABLE 1

Chemotaxis Parameters for MTLn3 Cells

Solution in the pipette	Chemotactic index[a]	Speed[a] (μm/min)
50 μM EGF	0.6 ± 0.15	0.82 ± 0.19
DPBS	0.15 ± 0.15	0.45 ± 0.08

[a] Mean ± SEM for eight cells. The computation of the parameters is described under Materials and Methods. Maximal chemotaxis occurs with an index of +1. Direct movement away from the pipette results in an index of −1. For both the chemotactic index and the speed, there is a significant difference ($P < 0.05$, Student t test) between the cells exposed to the gradient and the controls.

The above data suggested that stimulated protrusive activity was independent of any contact with the substratum and that the substratum might serve as a guide to concentrate actin polymerization at the leading edge during lamellipod extension. To concomitantly test these two hypotheses, we used two complementary experimental designs to visualize stimulated lamellipod extension of adherent cells under conditions that prevent the cells from making contacts with the substratum during extension: (i) adhesion-blocking peptides and (ii) patterned surfaces with nonadhesive and adhesive areas.

Adhesion-blocking peptides neither inhibit protrusion nor affect the shape of the protrusion. As expected, the GRGDSP peptide, which blocks the vitronectin receptor(s) [26, 59], inhibited initial MTLn3 cell attachment and spreading on vitronectin, while the GRADSP control peptide had no effect (data not shown). To selectively examine the role of adhesion in

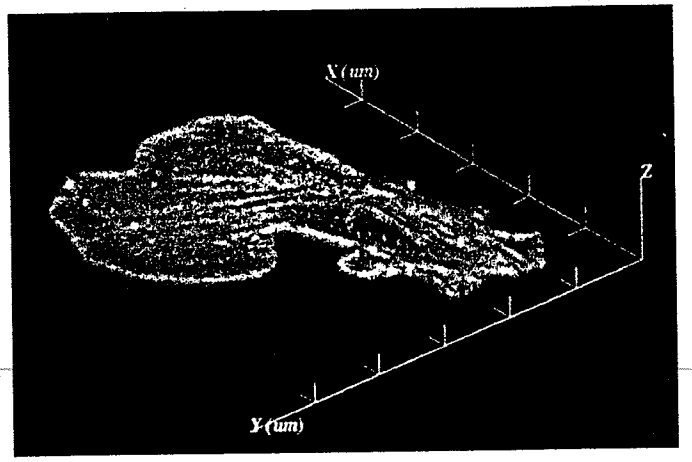

FIG. 2. F-actin accumulates at the edge of the spreading lamellipod in stimulated cells. MTLn3 cells were stimulated with EGF for 3 min, fixed, permeabilized, and stained for F-actin. Cells were imaged using confocal microscopy, and 3D reconstructions were achieved from Z-series using the Voxel view program with opacity proportional to F-actin staining. Note that the F-actin staining is concentrated at the edge of the expanding lamellipod rather than at the dorsal surface of the cell. Axis scale intervals, 10 μm.

EGF-stimulated lamellipod extension, MTLn3 cells were plated on vitronectin for 2 h in the absence of peptides. Following attachment and spreading, they were preincubated with either GRGDSP (adhesion blocking) or GRADSP (control) peptides for 10 min and then stimulated with EGF in the continued presence of the peptide (Fig. 6). Maximum lamellipod extension, as measured by an increase in total cell area [6], was slightly decreased in the presence of the GRGDSP peptide (approximately 70–80% of the response measured in the controls), but the kinetics of outward extension remained the same, with a maximum around 3–4 min after stimulation (Fig. 6). After the lamellipods had reached their maximum extension, however, those in the presence of blocking peptides retracted incrementally until the area of the cell was back to the prestimulus value. This retraction phase took place over the subsequent 5–6 min.

Protrusion occurs over nonadhesive surfaces. Since one cannot totally rule out the possibility that MTLn3 cells might use other receptors which are unaffected by GRGDSP peptides to make contact with the substratum during extension, or might have synthesized an alternative matrix molecule during attachment and then utilized it for spreading, an alternate method for preventing adhesive contacts with the substratum during lamellipod extension was used. Cells were plated on gold-coated glass coverslips designed with 10-μm-wide adhesive lane patterns (see Materials and Methods). Only the 10-μm-wide lanes support extracellular matrix adsorption and cell attachment, and any protrusions that the cells extend outside the lanes are over a nonadhesive surface [60, 61]. MTLn3 cells plated on these coverslips attached only to the lanes, as confirmed by anti-vitronectin staining (Fig. 7 and data not shown), and displayed an elongated shape (Fig. 8A). In most cases, the central mass of the cell bulged slightly over nonadhesive areas, leading to a maximum width of 12 μm on average (Fig. 8B, triangles). When cells plated on patterned coverslips were stimulated with EGF, their total area increased with the same kinetics and maximum extent as that of cells on a regular substratum. Stable lamellipod extension, however, occurred mainly in opposite directions along the lane of adhesive substratum (Fig. 8A). Digital analysis showed a dramatic extension in cell length which paralleled the increase in total cell area, reaching a maximum around 3–4 min after EGF stimulation and then plateauing (Fig. 8, diamonds). Analysis of the central width of the cells indicated that they became thinner as they stretched in opposite directions over their length (Fig. 8B, triangles). Quantitation of the maximum width (Fig. 8B, squares) indicated that before stimulation it reflected the central area. After stimulation, however, the extension of lamellipods over the nonadhesive surface led to the lamellipods becoming the widest areas of the cell, with an average maximum distance of 5 μm off the lane (Fig. 8B, squares). This extension off the lane peaked 3–4 min after EGF stimulation and then the maximum width decreased back to the value before stimulation. This decrease occurred incrementally over the course of 5 to 6 min, similar to what was observed for cells stimulated on vitronectin in presence of the GRGDSP peptide (compare inset in Figs. 8B and 6). The ability of the cells to extend laterally over the nonadhesive substratum was confirmed by fluorescence microscopy using rhodamine-labeled phalloidin to stain the F-actin in the cells and anti-vitronectin antibodies to stain the lanes of adhesive surface (Fig. 7).

These results confirmed that lamellipod extension is independent of any contact with the substratum and showed that preventing any contact with the substratum during lamellipod extension does not affect the shape of the protrusion which remains in the form a broad flat lamellipod. However, the extent of the protrusion may be slightly affected and the resulting lamellipod is unstable and retracts rapidly.

Chemoattractant-Induced Redistribution of Focal Contacts

As rapid, direct chemotactic responses have previously only been demonstrated for rapidly moving cells which have relatively weak adhesion to the substratum, it was important to confirm that the adhesive contacts of MTLn3 cells are similar to those found in

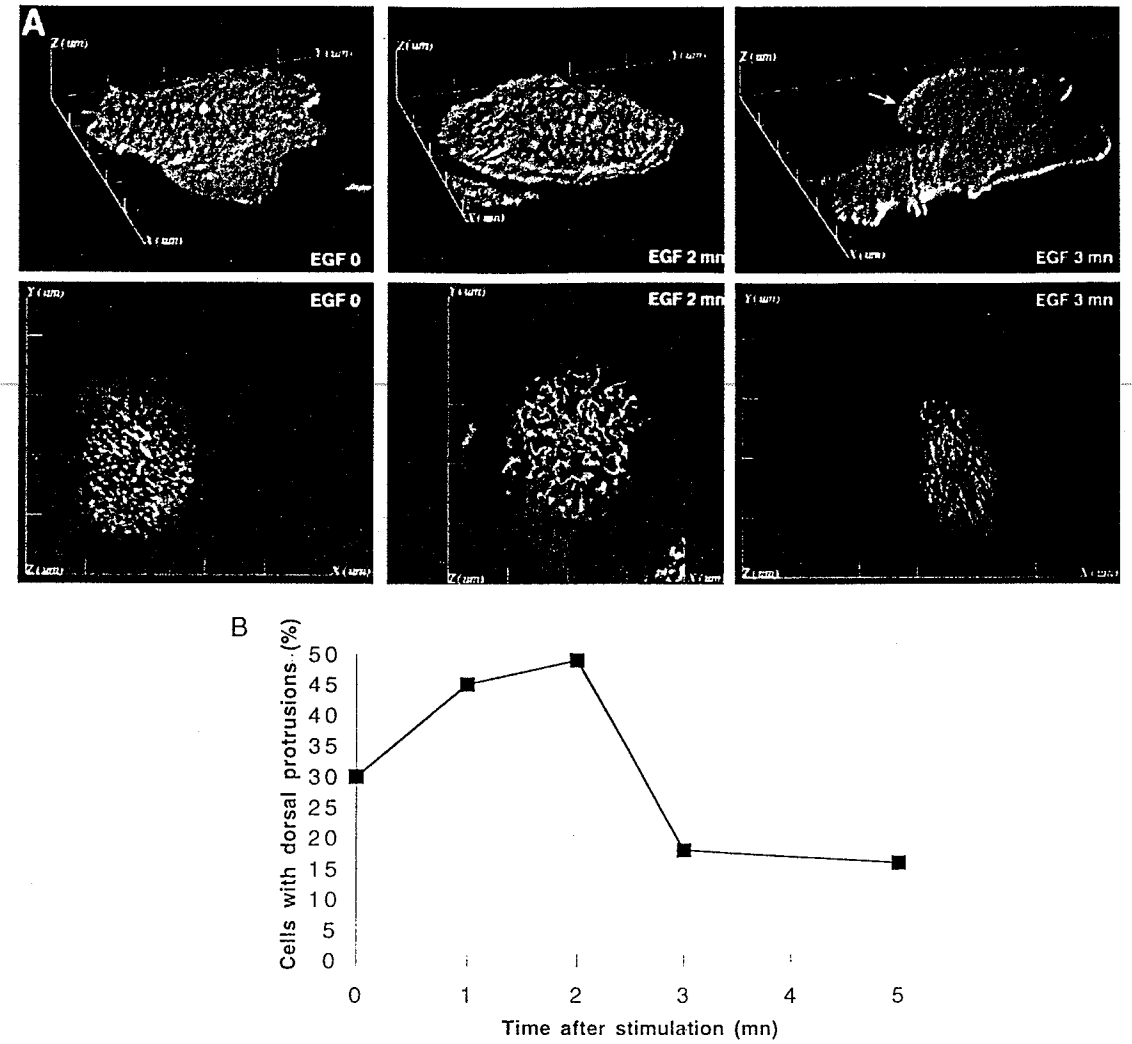

FIG. 3. Kinetics of protrusive activity on the dorsal surface of cells adhering to a substratum. Adherent MTLn3 cells were stimulated with EGF and then fixed, permeabilized, and stained with rhodamine-labeled phalloidin. (A) 3D reconstructions from confocal Z-series of representative adherent MTLn3 cells with opacity set to reveal the outer cortex of the cell, either unstimulated (EGF0) or 2 and 3 min after EGF stimulation (EGF2 and EGF3, respectively). (Top) Elevation view of the whole cells; (bottom) corresponding view from above the dorsal surface. Note the protrusions on the dorsal surface after 2 min, which are gone by 3 min. (Arrow) Lamellipod extension; axis scale intervals, 10 μm. (B) Quantitation of the number of cells with protrusions on their dorsal surface after EGF stimulation. The percentage of cells with protrusive activity on the dorsal surface was evaluated using regular fluorescence, from a minimum of 100 cells per time point.

other epithelial and mesenchymal cells. Using the upshift assay, lamellipod extension and changes in cell–substratum contacts were monitored using interference reflection microscopy (IRM). Figure 9 presents a representative IRM sequence. Adherent MTLn3 cells display typical areas of close contacts (gray areas) and discrete focal contacts (dark elongated spots, identified as described in Ref. [41]). The initial arrangement of focal contacts clearly is consistent with observations of randomly moving fibroblasts and other highly adherent cells. EGF stimulation triggered the rapid extension of a broad, flat lamellipod. This extension was maximal 3–4 min after stimulation and was accompanied by the formation of close contacts in the newly extended lamellipod (Fig. 9). After 5 min, new focal contacts were recognizable as intense dark spots in the newly extended area, and they increased in size over the course of 14 min. Simultaneously, many of the previously existing large focal contacts were remodeled: some became more diffuse and were no longer visible after 14 min, while those located at the rear were dragged and then at least partially disassembled, or left behind, as the cell retracted its tail (stars, Fig. 9). Thus, MTLn3 cells have adhesive contacts typical of highly adherent cells, and chemoattractant stimulation leads to a rearrangement of cell adhesive contacts, with an increase

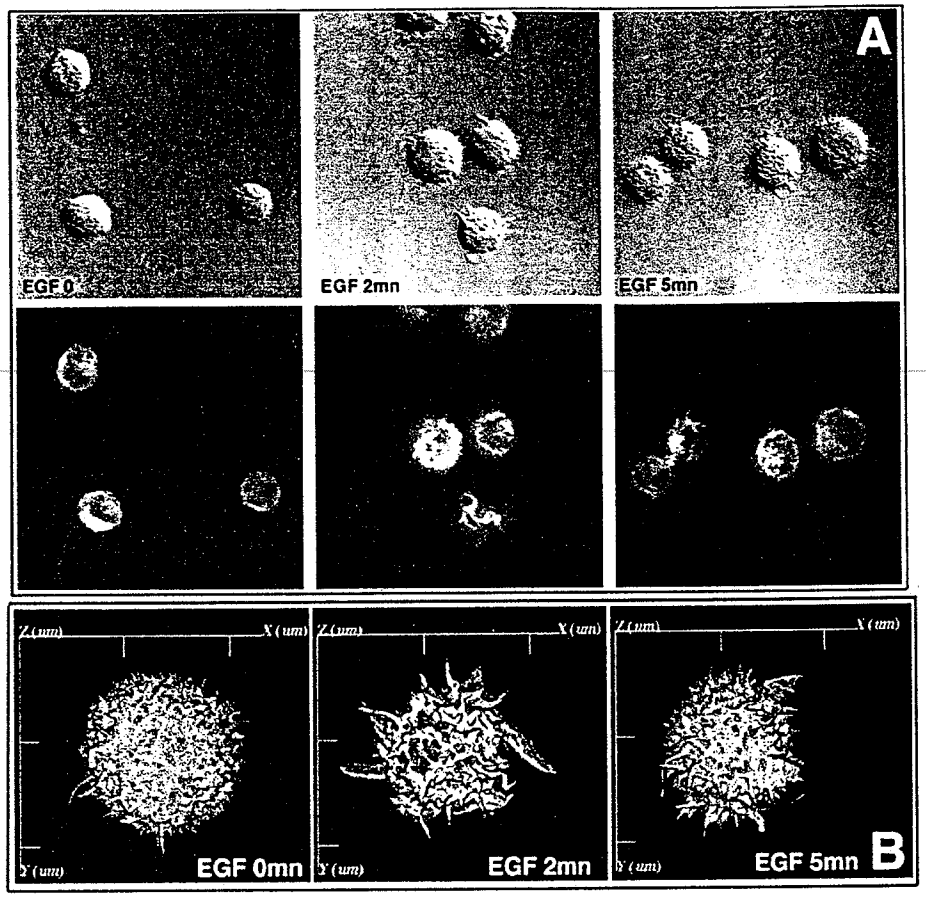

FIG. 4. EGF stimulates protrusive activity in cells in suspension. MTLn3 cells were stimulated in suspension with EGF and then fixed, permeabilized, and stained with rhodamine-labeled phalloidin. (A) Representative MTLn3 cells, either unstimulated (EGF0) or stimulated for 2 or 5 min (EGF2 and EGF5). (Top) DIC images; (bottom) corresponding F-actin fluorescence. (B) 3D reconstructions from confocal Z-series of representative cells after stimulation in suspension. Axis scale intervals, 10 μm.

in contacts in sites of new lamellipod extension and reduction in preexisting sites in the rear of the cell.

We then utilized talin as a marker to analyze chemoattractant-induced focal contact reorganization (Figs. 10A and 10B). Numerous new small focal contacts developed 5 min after stimulation and grew progressively to full, mature size by 20 min (Figs. 10C and 10D). These new focal contacts were not restricted to the margin of the lamellipod, but also developed back from the leading edge along the ventral surface of the cell. The mean number of focal contacts per cell increased significantly by 5 min after stimulation and peaked at 5–8 min (Fig. 11, circles). It then decreased to a steady level which was approximately twice that found in cells before stimulation. Concurrently, the mean length of the focal contacts decreased at 5 min after stimulation and then returned by 20 min to the length measured in unstimulated cells (Fig. 11, squares). These changes in number and size reflect the appearance and progressive growth of numerous new small focal contacts. Comparison of these kinetics with the kinetics of lamellipod extension demonstrates that the new focal contacts clearly appear after the lamellipod has reached maximal extension (dashed line).

DISCUSSION

Metastatic Tumor Cells Display True Chemotaxis

We demonstrate here that metastatic tumor cells display chemotaxis *in vitro* toward a point source comparable to what has been observed for ameboid cells such as *Dictyostelium* or neutrophils [55, 62]. This is the first direct demonstration of chemotactic ameboid movement by highly adherent cells towards a point source of growth factor. MTLn3 cells display a high chemotaxis index (i.e., 0.6), but, as is typical for epithelial or mesenchymal mammalian cells, move approximately 10 times more slowly than ameboid phagocytes, most probably because they display strong adhesion to the substratum, as reflected by the presence of numerous focal contacts and well-organized stress fibers. Net

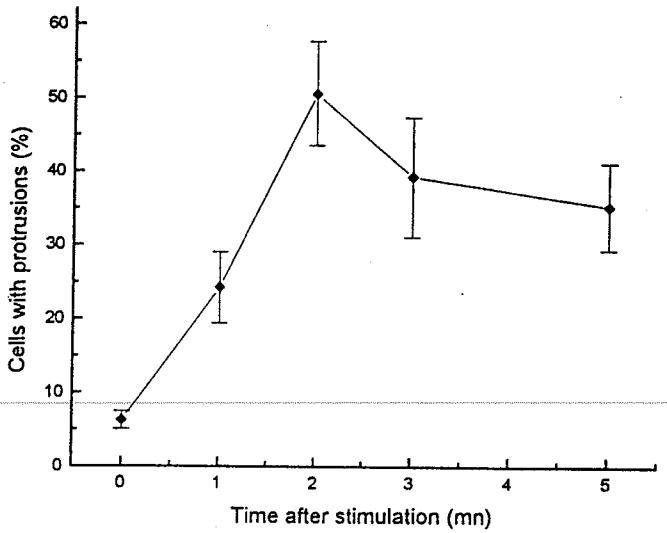

FIG. 5. Quantitation of cells showing protrusive activity in suspension after EGF stimulation. MTLn3 cells were stimulated in suspension with EGF and then fixed, permeabilized, and stained with rhodamine-labeled phalloidin. The percentage of cells with protrusions was evaluated using DIC. Results are the mean ± SEM of three different experiments where 268 to 497 cells were counted for each time point in each experiment.

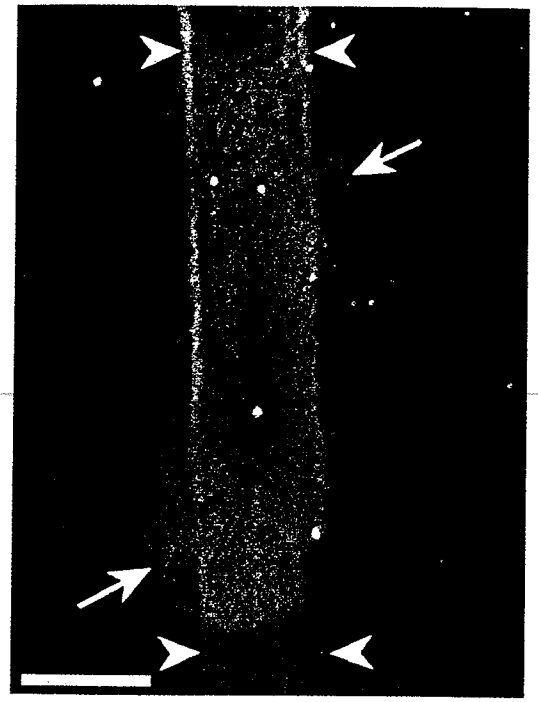

FIG. 7. EGF-stimulated lamellipod extension over a nonadhesive substratum. MTLn3 cells were plated on gold-coated glass coverslips which were patterned with hexadecanethiol and EG6-thiol to generate 10-μm lanes of adhesive substratum. Preparations were stimulated with EGF for 3 min, fixed, permeabilized, and double stained with rhodamine-labeled phalloidin to visualize the cell cytoskeleton and antibodies against vitronectin to visualize the adhesive lanes (arrowheads). Parallel images of single optical sections were taken with the confocal microscope and merged. (Green) Vitronectin staining; (red) F-actin staining. The cell shows prominent lamellipod extension over the nonadhesive surface (arrows). Bar, 10 μm.

movement toward the pipette was achieved through protrusion at the front of the cell, mainly in the form of extension of a broad lamellipod, combined with retraction at the rear. The extension and retraction can be modeled in the chemoattractant upshift experiment;

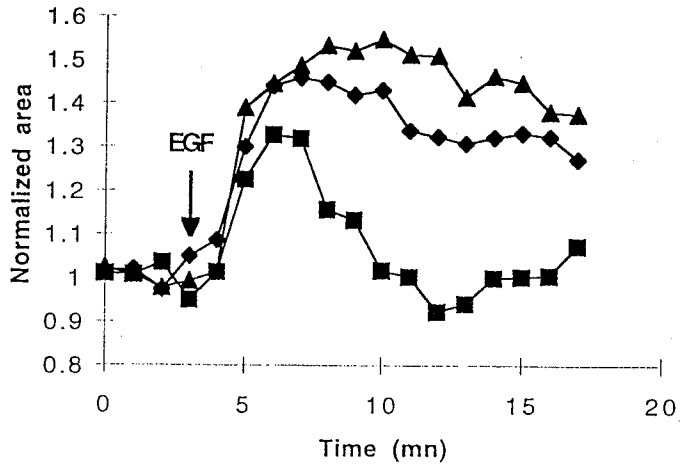

FIG. 6. MTLn3 cells display lamellipod extension in the presence of adhesion-inhibiting peptides. MTLn3 cells were plated for 2 h on vitronectin and stimulated with 5 nM EGF in regular medium (♦) or in the presence of 1.5 mM of the adhesion-inhibiting GRGDSP peptide (■) or the control GRADSP peptide (▲). Changes in cell shape were monitored using phase contrast microscopy and lamellipod extension was quantitated as described under Materials and Methods. Recording started 3 min prior to EGF stimulation (arrow). Results are the mean of 10 cells for each experiment (SEM < 10%).

homogeneous stimulation with EGF triggers a protrusive activity similar to what was observed in the pipette assay—broad lamellipod extension—and new contact formation. Similarly, the retraction phase can be seen using IRM in the upshift assay as the destabilization of preexisting contacts, retraction, and eventual ripping of the tail. Such a phenomenon has been previously described during random motion of fibroblasts [19, 22, 63].

Protrusive Activity Can Occur Independently of Any Contact with the Substratum

Our results unify studies performed on the chemotactic responses of a number of different highly adherent cell types with observations of randomly moving fibroblasts. We show that whatever the shape of the resulting protrusion (i.e., three-dimensional "ruffles" or flat, broad lamellipods), EGF-stimulated protrusive activity does not require contact with the substratum. Adherent cells can extend lamellipods over nonadhesive surfaces or in the presence of adhesion-blocking

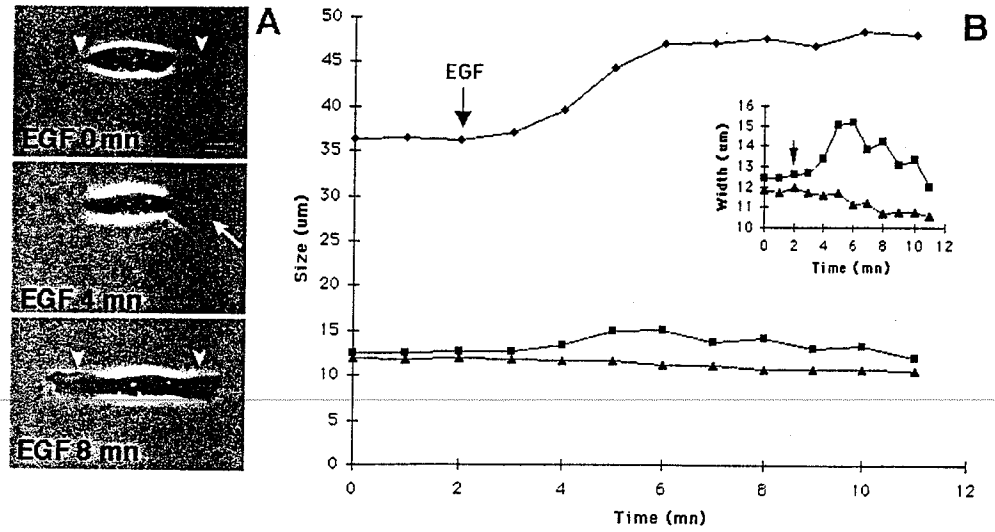

FIG. 8. MTLn3 cells extend lamellipods over a nonadhesive substratum. MTLn3 cells were plated on gold-coated glass coverslips which were patterned with hexadecanethiol and EG6-thiol to generate 10-μm lanes of adhesive substratum. They were stimulated with 5 nM EGF and changes in cell shape were monitored using phase contrast microscopy. Recording started 2 min prior to EGF stimulation (arrow). (A) Representative sequence of a cell stimulated on 10-μm lane-patterned coverslips. The cell is shown before stimulation (EGF0) and 4 and 8 min after stimulation (EGF4 and EGF8, respectively). Note the maximal lamellipod extension at 4 min (arrow). A net increase in cell length can be observed after 8 min (matched arrowheads). Bar, 10 μm. (B) Quantitation of the changes in cell shape after stimulation (mean for 14 cells, SEM < 10%). Three parameters were quantitated for each cell: maximum length (♦), maximum width (■), and central width (▲). (Inset) Narrowed scale showing more precisely the changes in the maximal width and central width over the same time course. Note that the maximal width increases after stimulation, showing that the cells are able to extend their lamellipods beyond the limits of the lane over the nonadhesive substratum (for a distance of about 2.5 μm on each side of the lane). This extension is followed by a rapid retraction, which brings back the maximal width of the cells within the limits of the adhesive lane (see A).

peptides and display dorsal protrusions after EGF stimulation. Furthermore, in an environment completely free of cell–substratum contacts, suspended cells exhibit high levels of protrusive activity after EGF stimulation. These observations are consistent with the idea that forces related to localized polymerization of actin are sufficient to drive protrusive activity [20, 64]. A number of elegant studies following the random movement of fibroblasts with interference reflection microscopy have noted that the leading edge of the lamellipod can be 100 nm or more above the surface of the coverslip [41, 65–67]. However, close contacts were rapidly formed by the extended lamellipod, which have been proposed to provide the adhesion required to transmit to the substratum the forces involved in the forward movement of the cytoplasm and advance of the leading lamella [19, 39, 41]. Thus, even though adhesion to a substratum is important to allow cells to spread normally during initial attachment, stimulated lamellipod extension is substratum independent.

Contact with the Substratum Stabilizes and Amplifies Protrusive Activity

Contact formation is not necessary for protrusive activity but is required for stabilizing the protrusion. We demonstrated this latter requirement using either cells stimulated in suspension or adherent cells extending protrusions over a nonadhesive substratum. Both types of experiments led to the same conclusions, i.e., that the kinetics and, to a lesser extent (see below), the magnitude of the protrusion are not affected by the absence of an adhesive substratum. In order for the protrusion to persist, however, an adhesive substratum was required. This is consistent with studies suggesting a correlation between the level of expression of matrix receptors and lamellipod stabilization during mesenchymal cell polarization in response to PDGF [23]. From the sequence of events that we observed, it appears that the establishment of new focal contacts may not be the primary adhesive event occurring to stabilize the extension. According to the kinetics of our IRM studies, primary stabilization of the lamellipod is correlated with the formation of close contacts. It remains, however, still unclear if close contacts are necessary *and* sufficient for further maintenance of the extension or if long-term stabilization requires focal contact formation. The focal contacts could be involved more in the process of motility itself, by generating traction forces necessary to pull the cell body forward to resume net movement [41, 68].

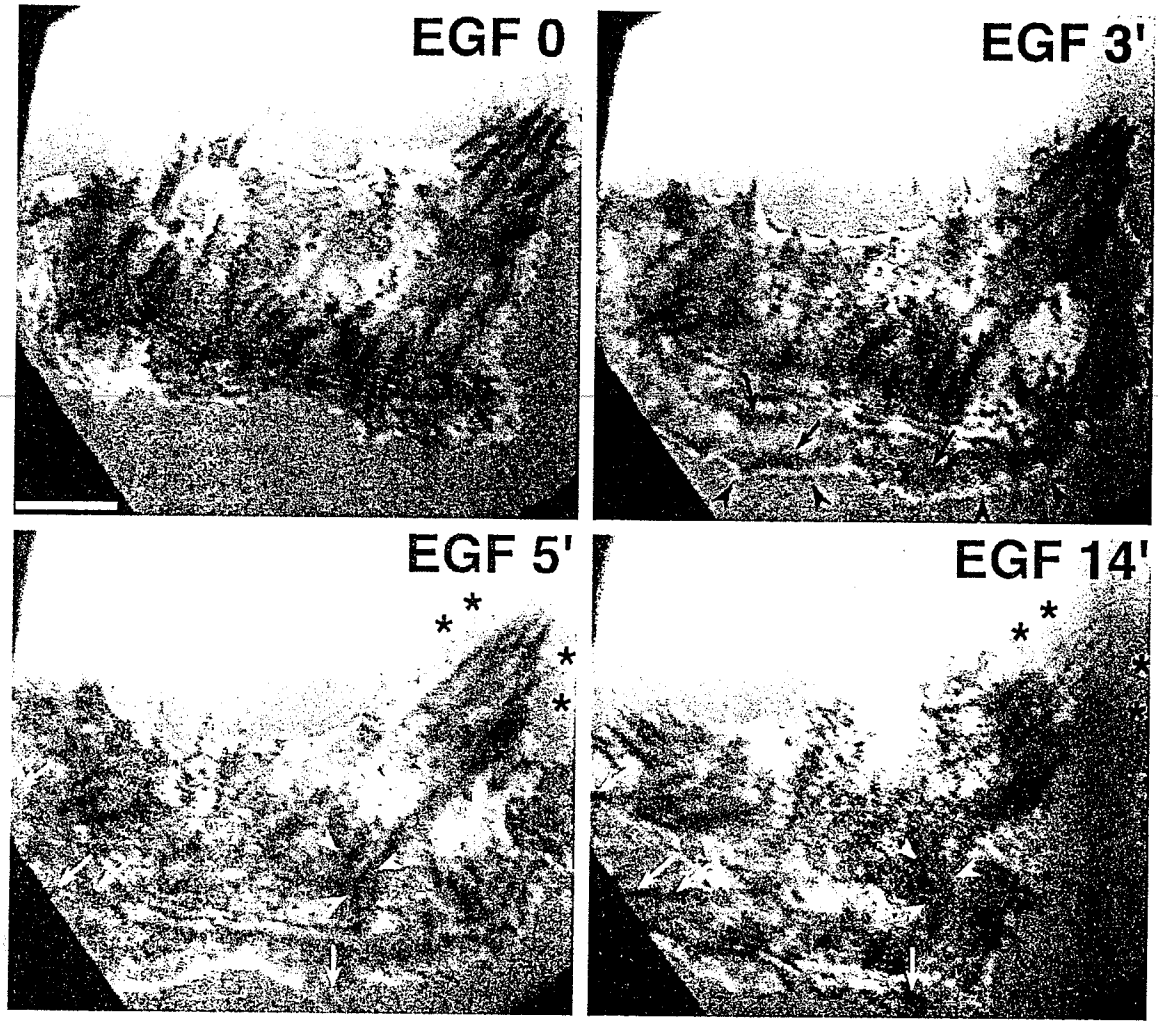

FIG. 9. IRM analysis of lamellipod extension and modifications of cell–substratum contacts after a homogeneous upshift in EGF. The sequence shows representative images of the same cell immediately before and up to 14 min after EGF stimulation (time is indicated as minutes after stimulation). EGF stimulation triggered a lamellipod extension which was maximum around 3 min after stimulation (black arrowheads). This extension was accompanied by the establishment of close contacts in the newly extended area (black arrows). After 5 min, new focal contacts formed, which increased in size over the course of the experiment (white arrows). Previously existing focal contacts were remodeled; some became diffuse and were no longer visible after 14 min (white arrowheads). Focal contacts at tail disassembled during tail retraction (stars). Bar, 10 μm.

Although our results show that continuous contact with the substratum is not necessary for lamellipod extension, such contact may amplify lamellipod extension. As stated above, contact with the substratum during the extension does not affect the kinetics of the lamellipod extension in adherent cells. The amplitude of the protrusion, however, was decreased by 20–30% when contacts with the substratum were prevented by adhesion-inhibiting peptides. It is now well established that signals can be transmitted from the substratum to the inside of the cell, affecting many cell processes such as cell division, differentiation, apoptosis, or motility [23, 30, 31, 69, 70]. One of the major families of membrane molecules involved in these processes is the family of integrin receptors [30, 31]. Many of these receptors have been shown to trigger downstream signaling inside the cell, and some of them have been shown to affect actin polymerization and lamellipod extension, although the exact pathways involved are presently still unclear [36–38]. In our experiments, it is conceivable that contact of the vitronectin receptor(s) with the ligand triggers a signal which leads to the potentiation of actin polymerization and subsequent increase in the level of protrusive activity. Indeed, it has been shown that activation of the integrin $\alpha_v\beta_3$, which is one of the major vitronectin receptors in epithelial cells, can trigger a downstream signal which will affect actin polymerization and cell motility through protein kinase C activation [37].

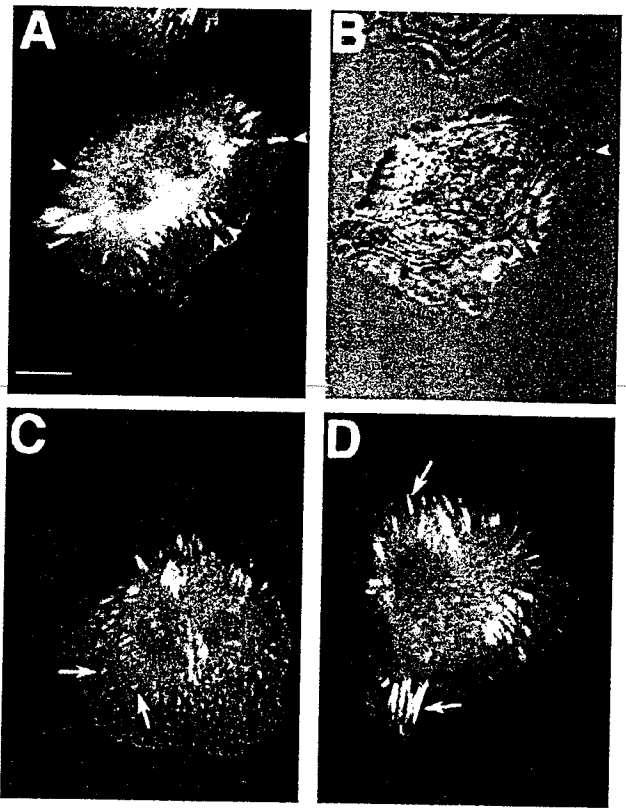

FIG. 10. EGF stimulation triggers focal contact assembly. MTLn3 cells were stimulated with EGF, fixed, permeabilized, and immunostained with antibodies against talin to visualize focal contacts and imaged using confocal microscopy. (A) Unstimulated MTLn3 cell stained for talin. Note large preexisting focal contacts (arrowheads). (B) Same cell as viewed by IRM. Note that the talin-based focal contact pattern matches exactly the focal contact pattern revealed by IRM (matching arrowheads in A and B). (C) Numerous newly formed focal contacts are visible 5 min after EGF stimulation (arrows). (D) 20 min after EGF stimulation, the new focal contacts have grown to the size of mature focal contacts (arrows). Bar, 10 μm.

The Prestimulus Status of the Cell Conditions the Shape of the Lamellipod

One of the intriguing results of our study is that adherent cells which protrude over a nonadhesive substratum still extend a flat broad lamellipod. Earlier work on cytokine-stimulated pseudopodial protrusion had led to the idea that pseudopodia might act as sensers which use contacts with the substrate to guide the protrusive activity and "help determine the vectorial direction of locomotion" [49]. We demonstrate here, however, that while stimulated adherent cells show some extent of protrusive activity over their dorsal surface, the major protrusive event remains the extension of a broad flat lamellipod, whether or not in contact with the substratum. Similarly, cells adhering over a patterned substrate preferentially extend over the adhesive lanes, resulting in an extremely elongated shape. These results suggest that the initial "adhesive" status of the cell, i.e., in contact or not with a substratum, influences the shape and the location of the protrusion to be generated after stimulation. Consistent with the hypothesis that spreading of the cell on the substratum prior to stimulation, rather than simple contact with the substrate, is mandatory for the two-dimensional extension of a flat lamellipod, we have seen that cells which are adherent but not well spread behave mostly like cells in suspension after EGF stimulation (i.e., sending numerous protrusions, data not shown). It is conceivable that the special conformation of the actin meshwork in the lamella of spread adherent cells [20, 64], as well as the fact that this part of the cell is already in close contact with the substratum (which could locally potentiate the stimulated protrusive activity, see above), allows for a more focused burst of actin polymerization in the lamella as compared with other parts of the cell. The maintenance of a spread shape might indeed require an "active" leading edge, which potentially constitutes a specific intracellular molecular compartment that would be highly receptive to signal transduction in general and more particularly to EGF-mediated stimulation of actin polymerization.

Some degree of three-dimensional protrusive activity was observed on the dorsal surface of cells after EGF stimulation, but it was only transient and disappeared by the time the lamellipod had reached maximal extension. Concomitant stabilization and amplification of the protruding activity at the leading edge as the lamellipod extends over the substratum could generate membrane extension, which in turn might create sufficient tension to inhibit protrusions over the dorsal surface. On the other hand, dorsal protrusions may be transient because they do not get stabilized by contact with the substratum. The first explanation is however more consistent with our results because those protrusions on the dorsal surface of stimulated adherent cells are shorter lived than protrusions on cells in suspension, disappearing within a single minute interval.

In conclusion, the results presented in this paper support the following model of tumor cell migration through loose connective tissue during metastasis [see also Refs. 54 and 71]: (i) upon exposure to a gradient of chemoattractant such as EGF, lamellipod extension from sites of interaction with matrix is initiated. This extension does not require continuous contact with matrix molecules. Indeed, matrix proteolysis by tumor cells may accentuate the need to extend lamellipods across gaps in the fiber components. (ii) Cell extensions that do contact matrix fibers are then stabilized, while older contact sites (such as those at the rear of the cell) are destabilized resulting in forward movement of the cell. (iii) The net result is a consistent progression through the extracellular matrix that facilitates tumor cell dispersal.

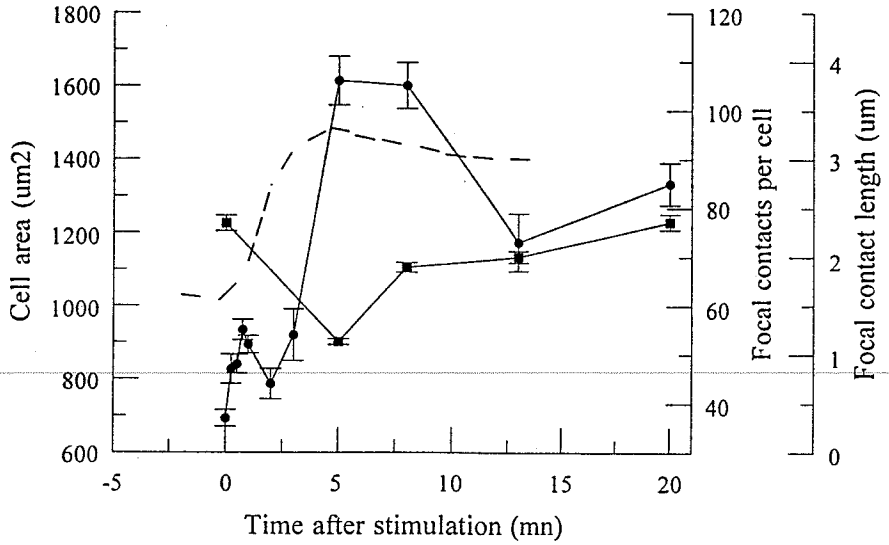

FIG. 11. Focal contact distribution following EGF stimulation. The number (●) and the length (■) of talin-containing focal contacts were assessed for individual cells at each time point on single optical sections taken with the confocal microscope. The results for focal contact numbers are the sum of two comparable experiments, and each point shows the mean (±SEM) for 15 to 55 cells. The size of the focal contacts was evaluated on four representative cells for each time point. Dashed line, kinetics of lamellipod extension after EGF stimulation. Lamellipod extension is shown as an increase in the total area of the cells (50 cells, SEM < 5%).

The authors acknowledge the Analytical Imaging Facility at the Albert Einstein College of Medicine and particularly Michael Cammer for skillful help on microscopy and image analysis. The authors also acknowledge Dr. C. J. Chang from the Biostat Core at Albert Einstein College of Medicine for help on statistical analysis, Dr. Milan Mrksich for discussion regarding the nonadhesive substrata, Dr. Dong Qin for preparing special patterned samples, and members of the lab group meetings for helpful discussion. A link to the movie that was used to generate Figure 1 can be found on the bibliography pages of the Analytical Image Facility of the Albert Einstein College of Medicine web server (AECOM URL: http://www.aecom.yu.edu). This work was supported by grants USAMRDC 2466 (JES), GM38511 (JSC), and GM30367 (GMW). J.S. is supported by an Established Scientist Award from the New York City Affiliate of the American Heart Association.

REFERENCES

1. Gutman, M., and Fidler, I. J. (1995). Biology of human colon cancer metastasis. *World J. Surgery* **19,** 226–234.
2. Kohn, E. C., and Liotta, L. A. (1995). Molecular insights into cancer invasion: strategies for prevention and intervention. *Cancer Res.* **55,** 1856–1862.
3. Lawrence, J. A., and Steeg, P. S. (1996). Mechanisms of tumor invasion and metastasis. *World J. Urol.* **14,** 124–130.
4. Chicoine, M. R., and Silbergeld, D. L. (1995). The in vitro motility of human glioma increases with increasing grade of malignancy. *Cancer* **75,** 2904–2909.
5. Verschueren, H., Van der Taelen, I., Dewit, J., De Braekeleer, J., and De Baetselier, P. (1994). Metastatic competence of BW5147 T-lymphoma cell lines is correlated with in vitro invasiveness, motility and F-actin content. *J. Leukocyte Biol.* **55,** 552–556.
6. Segall, J. E., Tyerech, S., Boselli, L., Masseling, S., Helft, J., Chan, A., Jones, J., and Condeelis, J. (1996). EGF stimulates lamellipod extension in metastatic mammary adenocarcinoma cells by an actin-dependent mechanism. *Clin. Exp. Metastasis* **14,** 61–72.
7. Xie, H., Turner, T., Wang, M. H., Singh, R. K., Siegal, G. P., and Wells, A. (1995). In vitro invasiveness of DU-145 human prostate carcinoma cells is modulated by EGF receptor-mediated signals. *Clin. Exp. Metastasis* **13,** 407–419.
8. Pedersen, P. H., Ness, G. O., Engebraaten, O., Bjerkvig, R., Lillehaug, J. R., and Laerum, O. D. (1994). Heterogeneous response of the growth factors (EGF, PDGF (bb), TGF-alpha, bFGF, IL2) on glioma spheroid growth, migration and invasion. *Int. J. Cancer* **56,** 255–261.
9. Kundra, V., Soker, S., and Zetter, B. R. (1994). Excess early signaling activity inhibits cellular chemotaxis toward PDGF-BB. *Oncogene* **9,** 1429–1435.
10. Matsumoto, K., Matsumoto, K., Nakamura, T., and Kramer, R. H. (1994). Hepatocyte growth factor/scatter factor induces tyrosine phosphorylation of focal adhesion kinase ($p125^{FAK}$) and promotes migration and invasion by oral squamous cell carcinoma cells. *J. Biol. Chem.* **269,** 31807–31813.
11. Klijn, J. G., Look, M. P., Portengen, H., Alexieva-Figusch, J., VanPutten, W. L., and Foekens, J. A. (1994). The prognostic value of epidermal growth factor receptor (EGF-R) in primary breast cancer: results from a 10 year follow-up study. *Breast Cancer Res. Treat.* **29,** 73–83.
12. Lewis, S., Locker, A., Todd, J. H., Bell, J. A., Nicholson, R., Elston, C. W., Blamey, R. W., and Ellis, I. O. (1990). Expression of epidermal growth factor receptor in breast carcinoma. *J. Clin. Path.* 43, 385–389.
13. Nicholson, S., Richard, J., Sainsbury, C., Halcrow, P., Kelly, P., Angus, B., Wright, C., Henry, J., Farndon, J. R., and Harris, A. L. (1991). Epidermal growth factor receptor (EGF-r): Results of a 6-year follow-up study in operable breast cancer with emphasis on the node negative subgroup. *Br. J. Cancer* **63,** 146–150.

14. Battaglia, F., Scambia, G., Rossi, S., Panici, P. B., Bellantone, R., Polizzi, G., Querzoli, P., Negrini, R., Iacobelli, S., Crucitti, F., *et al.* (1988). Epidermal growth factor receptor in human breast cancer: correlation with steroid hormone receptors and axillary lymph node involvement. *Eur. J. Cancer Clin Oncol.* **24,** 1685–1690. [published erratum appears *in Eur. J. Cancer Res. Clin Oncol.* **25,** 577, 1989]
15. Toi, M., Osaki, A., Yamada, H., and Toge, T. (1991). Epidermal growth factor receptor expression as a prognostic indicator in breast cancer. *Eur. J. Cancer* **27,** 977–980.
16. Condeelis, J. (1998). The biochemistry of animal cell crawling. *In* "Motion Analysis of Living Cells" (D. Soll, Ed.), Wiley-Liss, Inc., 85–100.
17. Downey, G. P. (1994). Mechanisms of leukocyte motility and chemotaxis. *Curr. Opin. Immunol.* **6,** 113–124.
18. Caterina, M. J., and Devreotes, P. N. (1991). Molecular insights into eukaryotic chemotaxis. *FASEB J.* **5,** 3078–3085.
19. Lauffenburger, D. A., and Horwitz, A. F. (1996). Cell migration: A physically integrated molecular process. *Cell* **84,** 359–369.
20. Mitchison, T. J., and Cramer, L. P. (1996). Actin-based cell motility and cell locomotion. *Cell* **84,** 371–379.
21. Palecek, S. P., Loftus, J. C., Ginsberg, M. H., Lauffenburger, D. A., and Horwitz, A. F. (1997). Integrin-ligand binding properties govern cell migration speed through cell-substratum adhesiveness. *Nature* **385,** 537–541.
22. Palecek, S. P., Schmidt, C. E., Lauffenburger, D. A., and Horwitz, A. F. (1996). Integrin dynamics on the tail region of migrating fibroblasts. *J. Cell Sci.* **109,** 941–951.
23. Appeddu, P. A., and Shur, B. D. (1994). Control of stable lamellipodia formation by expression of cell surface beta 1,4-galactosyltransferase cytoplasmic domains. *J. Cell Sci.* **107,** 2535–2545.
24. Abercrombie, M., Heaysman, J. E. M., and Pegrum, S. M. (1970b). The locomotion of fibroblasts in culture. I. Movements of the leading edge. *Exp. Cell Res.* **59,** 393–398.
25. Hendey, B., and Maxfield, F. R. (1993). Regulation of neutrophil motility and adhesion by intracellular calcium. *Blood Cells* **19,** 143–161.
26. Izzard, C. S., Radinsky, R., and Culp, L. A. (1986). Substratum contacts and cytoskeletal reorganization of BALB/c 3T3 cells on a cell-binding fragment and heparin-binding fragments of plasma fibronectin. *Exp. Cell Res.* **165,** 320–336.
27. Woods, A., Couchman, J. R., Johansson, S., and Hook, M. (1986). Adhesion and cytoskeletal organization of fibroblasts in response to fibronectin fragments. *EMBO J.* **5,** 665–670.
28. Gehlsen, K. R., Argraves, W. S., Pierschbacher, M. D., and Ruoslahti, E. (1988). Inhibition of in vitro tumor cell invasion by Arg-Gly-Asp-containing synthetic peptides. *J. Cell Biol.* **106,** 925–930.
29. Nobes, C., and Hall, A. (1995). Rho, rac, and Cdc42 GTPases regulate the assembly of multimolecular focal complexes associated with actin stress fibers, lamellipodia, and filipodia. *Cell* **81,** 53–62.
30. Dedhar, S. (1995). Integrin mediated signal transduction in oncogenesis: An overview. *Cancer Metastasis Rev.* **14,** 165–172.
31. Parsons, J. T. (1996). Integrin-mediated signaling: regulation by protein tyrosine kinases and small GTP-binding proteins. *Curr. Opin. Cell Biol.* **8,** 146–152.
32. Hynes, R. O. (1992). Integrins: Versatility, modulation, and signaling in cell adhesion. *Cell* **69,** 11–25.
33. Schwartz, M. A., Schaller, M. D., and Ginsberg, M. H. (1995). Integrins: Emerging paradigms of signal transduction. *Annu. Rev. Cell Dev. Biol.* **11,** 549–599.
34. Yamada, K. M., and Geiger, B. (1997). Molecular interactions in cell adhesion complexes. *Curr. Opin. Cell Biol.* **9,** 76–85.
35. Burridge, K., Turner, C. E., and Romer, L. H. (1992). Tyrosine phosphorylation of paxillin and pp125^{FAK} accompanies cell adhesion to extracellular matrix: a role in cytoskeletal assembly. *J. Cell Biol.* **119,** 893–903.
36. Balzac, F., Retta, S. F., Albini, A., Melchiorri, A., Koteliansky, V. E., Geuna, M., Silengo, L., and Tarone, G. (1994). Expression of beta 1B integrin isoform in CHO cells results in a dominant negative effect on cell adhesion and motility. *J. Cell Biol.* **127,** 557–565.
37. Klemke, R. L., Yebra, M., Bayna, E. M., and Cheresh, D. A. (1994). Receptor tyrosine kinase signaling required for integrin alpha v beta 5-directed cell motility but not adhesion on vitronectin. *J. Cell Biol.* **127,** 859–866.
38. Chrzanowska-Wodnicka, M., and Burridge, K. (1996). Rho-stimulated contractility drives the formation of stress fibers and focal adhesions. *J. Cell Biol.* **133,** 1403–1415.
39. Ingram, V. M. (1969). A side view of moving fibroblasts. *Nature* **222,** 641–644.
40. Abercrombie, M., Heaysman, J. E. M., and Pegrum, S. M. (1970). The locomotion of fibroblasts in culture. II. "Ruffling." *Exp. Cell Res.* **60,** 437–444.
41. Izzard, C. S., and Lochner, L. R. (1980). Formation of cell-to-substrate contacts during cell motility: An interference-reflection study. *J. Cell Sci.* **42,** 81–116.
42. Harris, A., and Dunn, G. (1972). Centripetal transport of attached particles on both surfaces of moving fibroblasts. *Exp. Cell. Res.* **73,** 519–523.
43. Heath, J. P., and Peachey, L. D. (1989). Morphology of fibroblasts in collagen gels: A study using 400 keV electron microscopy and computer graphics. *Cell Motil. Cytoskel.* **14,** 382–392.
44. Rovensky, Y. A., Bershadsky, A. D., Givargizov, E. I., Obolenskaya, L. N., and Vasiliev, J. M. (1991). Spreading of mouse fibroblasts on the substrate with multiple spikes. *Exp. Cell Res.* **197,** 107–112.
45. Huttenlocher, A., Ginsberg, M. H., and Horwitz, A. F. (1996). Modulation of cell migration by integrin-mediated cytoskeletal linkages and ligand-binding affinity. *J. Cell Biol.* **134,** 1551–1562.
46. Aznavoorian, S., Stracke, M. L., Parsons, J., McClanahan, J., and Liotta, L. A. (1996). Integrin alphav-beta3 mediates chemotactic and haptotactic motility in human melanoma cells through different signaling pathways. *J. Biol. Chem.* **271,** 3247–3254.
47. Lallier, T. (1996). Migration and adhesion assays. *Methods Cell Biol.* **51,** 285–299.
48. Komai-Koma, M., and Wilkinson, P. C. (1997). Locomotor properties of human germinal centre B cells: Activation by anti-CD40 and IL4 allows chemoattraction by anti-immunoglobulin. *Immunology* **90,** 23–29.
49. Guirguis, R., Margulies, I., Taraboletti, G., Schiffmann, E., and Liotta, L. A. (1987) Cytokine-induced pseudopodial protrusion is coupled to tumor cell migration. *Nature* **329,** 261–263.
50. Zicha, D., and Dunn, G. A. (1995). Are growth factors chemotactic agents? *Exp. Cell Res.* **221,** 526–529.
51. Segall, J. E. (1988). Quantification of motility and area changes in Dictyostelium discoideum amoebae in response to chemoattractants. *J. Muscle Res. Cell Motil.* **9,** 481–490.
52. Cox, D., Wessels, D., Soll, D. R., Hartwig, J., and Condeelis, J. (1996). Re-expression of ABP-120 rescues cytoskeletal, motility, and phagocytosis defects of ABP-120$^-$ Dictyostelium mutants. *Mol. Biol. Cell* **7,** 803–823.

53. Kumar, A., and Whitesides, G. M. (1993). Features of gold having micrometer to centimeter dimensions can be formed through a combination of stamping with elastomeric stamp and alkanethiol "ink" followed by chemical etching. *Appl. Phys. Lett.* **63,** 2002–2004.

54. Prime, K. L., and Whitesides, G. M. (1993). Adsorption of proteins onto surfaces containing end-attached oligo(ethylene glycol): A model system using self-assembled monolayers. *J. Am. Chem. Soc.* **115,** 10714–10721.

55. Devreotes, P. M., and Zigmond, S. H. (1988). Chemotaxis in eukaryotic cells: A focus on leukocytes and Dictyostelium. *Annu. Rev. Cell Biol.* **4,** 649–686.

56. Segall, J. E., and Gerisch, G. (1989). Genetic approaches to cytoskeleton function and the control of cell motility. *Curr. Opin. Cell Biol.* **1,** 44–50.

57. Wyckoff, J. B., Insel, L., Khazaie, K., Lichtner, R., Condeelis, J. S., and Segall, J. E. Suppression of ruffling by EGF in chemotactic cells. Submitted for publication.

58. Chan, A. Y., Raft, S., Bailly, M., Wyckoff, J. B., Segall, J. E., and Condeelis, J. E. (1998). EGF stimulates actin nucleation at the tip of the lamellipod in mammary adenocarcinoma cells. *J. Cell Science,* **111,**199–211.

59. Pierschbacher, M. D., and Ruoslahti, E. (1987). Influence of stereochemistry of the sequence Arg-Gly-Asp-Xaa on binding specificity in cell adhesion. *J. Biol. Chem.* **262,** 17294–17298.

60. Singhvi, R., Kumar, A., Lopez, G. P., Stephanopoulos, G. N., Wang, D. I. C., Whitesides, G. M., and Ingber, D. E. (1994). Engineering cell shape and function. *Science* **264,** 696–698.

61. Chen, C. S., Mrksich, M., Huang, S., Whitesides, G. M., and Ingber, D. E. (1997). Geometric control of cell life and death. *Science* **276,** 1425–1428.

62. Wessels, D., Vawter-Hugart, H., Murray, J., and Soll, D. (1994). Three-dimensional dynamics of pseudopod formation and the regulation of turning during the motility cycle of Dictyostelium. *Cell Motil. Cytoskel.* **27,** 1–12.

63. Chen, W.-T. (1981). Mechanisms of retraction and the trailing edge during fibroblast movement. *J. Cell Biol.* **90,** 187–200.

64. Condeelis, J. (1993). Life at the leading edge: the formation of cell protrusions. *Annu. Rev. Cell Biol.* **9,** 411–444.

65. Couchman, J. R., and Rees, D. A. (1979). The behavior of fibroblasts migrating from chicken heart explants: Changes in adhesion, locomotion and growth, and in the distribution of actomyosin and fibronectin. *J. Cell Sci.* **39,** 149–165.

66. Haemmerli, G., Sträuli, P., and Ploem, J. S. (1980). Cell-to-substrate adhesions during spreading and locomotion of carcinoma cells. *Exp. Cell Res.* **128,** 249–256.

67. Bereiter-Hahn, J., Strohmaier, R., Kunzenbacher, I., Beck, K., and Voth, M. (1981). Locomotion of Xenopus epidermis cells in primary culture. *J. Cell Sci.* **52,** 289–311.

68. Akasaka, T., van Leeuwen, R. L., Yoshinaga, I. G., Mihm, M. C., Jr., and Byers, H. R. (1995). Focal adhesion kinase (p125FAK) expression correlates with the motility of human melanoma cell lines. *J. Invest. Derm.* **105,** 104–108.

69. Hall, C. L., Wang, C., Lange, L. A., and Turley, E. A. (1994). Hyaluronan and the hyaluronan receptor RHAMM promote focal adhesion turnover and transient tyrosine kinase activity. *J. Cell Biol.* **126,** 575–588.

70. Leavesley, D. I., Schwartz, M. A., Rosenfeld, M., and Cheresh, D. A. (1993). Integrin beta1- and beta3-mediated endothelial cell migration is triggered through distinct signaling mechanisms. *J. Cell Biol.* **121,** 163–170.

71. Mandeville, J. T., Lawson, M. A., and Maxfield, F. R. (1997). Dynamic imaging of neutrophil migration in three dimensions: Mechanical interactions between cells and matrix. *J. Leukocyte Biol.* **61,** 188–200.

Received August 11, 1997
Revised version received December 15, 1997